

Methodological add-ons to a non-destructive, micro-CT-based taxonomic/morphometric analysis of characean remains

Réka Benyó-Korcsmáros^{1*}, Sándor Gulyás¹, Dániel Sebők², Dániel Benyó³, Péter Cseh¹, Pál Sümegi¹

¹University of Szeged, Department of Geology and Paleontology, Egyetem utca 2-6, 6722 Szeged, Hungary; e-mails: S.G. gulyas.sandor@geo.u-szeged.hu, P.C. cspeter@geo.u-szeged.hu, P.S. sumegi@geo.u-szeged.hu

²University of Szeged, Department of Applied and Environmental Chemistry, Interdisciplinary Excellence Centre, Rerrich Béla tér 1, 6720 Szeged, Hungary; e-mail: sebokd@chem.u-szeged.hu

³Institute of Plant Biology, Biological Research Centre, Temesvári krt. 62. 6726 Szeged, Hungary; e-mail: benyo.daniel@brc.hu

*corresponding author, e-mail: bkreka@geo.u-szeged.hu

Abstract

Ever since its introduction, computed tomography has come a long way. No longer is it merely a method that is used in clinical diagnostics, but it is becoming more and more popular among palaeontologists because it can be used to analyse both external and internal structures of fossil remains, such as small insects, snail shells and plant remains. The present study describes non-destructive analyses of Late Cretaceous and early Holocene charophyte gyrogonites by using the micro-CT technique, from sample preparation (embedding, fixing) to visualisation and assessment of images obtained. In addition to this non-destructive examination, we wished to test whether or not computed tomography could be used to examine the gyrogonites. Our preliminary results have made it clear that the micro-CT technique is worth employing for further research. It has proved possible to visualise the samples in 3D, rotate them, and observe them from different directions. By using the appropriate parameters, we have also been able to observe density differences between parts of characean remains and to study several important defining features of these.

Keywords: Characeae, computer tomography, gyrogonites

1. Introduction

Charophytes have proved increasingly important in reconstructions of palaeoenvironments, because, depending on species and environmental conditions, their fertilised female reproductive structures (oospores) might constitute a resistant structure that could fossilise. Such a structure is produced by calcification of the spiral cells surrounding the oospores, resulting in a so-called gyrogonite. However, intracellular calcification may be controlled by various genetic processes, and gyrogonite shape does not necessarily replicate that

of the inner structure (Soulié-Märsche & García, 2015).

The most widely used tool for studying gyrogonites is the scanning electron microscope (SEM) (Soulié-Märsche & García, 2015), which has the advantage of allowing an examination of very small details and patterns on the gyrogonite surface. To date, SEMs are available that allow examination of uncoated samples (i.e., no gold or carbon coating). However, encrustations need to be removed prior to any study of the internal structure.

An analytical method has to be found that allows examination of both external and internal

structures of samples without destroying them (Tafforeau et al., 2006). This is why the micro-CT technique was chosen. Beyond the non-destructive nature of this method, we wished to test whether or not computed tomography might prove of use in analysing gyrogonites.

2. Basics of computed tomography

Computed tomography (CT) was developed by combining and simultaneously using the techniques of X-ray imaging and computer science. Allan M. Cormack and Godfrey N. Hounsfield were awarded the Nobel Prize in Medicine for its development in 1979. It has been used almost exclusively as a branch of radiological diagnostics ever since its introduction (Hounsfield, 1973). However, because of technological development and increased financial resources, computed tomography is no longer a method used only in medical diagnostics and industry, but is also being increasingly widespread as a non-destructive method in basic and applied laboratory scientific research (Tafforeau et al., 2006).

Computed tomography is based on the measurement of different degrees of absorption of X-rays (Hounsfield, 1973). X-ray is a high-energetic, electromagnetic, ionizing radiation. The longer wavelength (and lower energy) part of its electromagnetic spectrum borders on ultraviolet radiation, called soft X-rays, while the shorter wavelength (higher energy) part borders on and partly overlaps with gamma rays, referred to as hard X-rays. The device that is used to produce X-rays artificially is an X-ray tube. When a high voltage is applied to the electrodes in the vacuum, the electrons leaving the cathode are accelerated towards the anode and then hit it. This process produces X-rays.

The electricity (IC, typically μA , mA) flowing through the cathode controls the number of electrons (intensity) leaving it, while the accelerator voltage (UA, typically kV) connected between the cathode and anode determines the hardness of the radiation.

Depending on the density of the object to be scanned, either soft radiation ($U = 30\text{--}50$ kV, e.g., organs in diagnostics or plastics in materials science) or hard radiation ($U > 100$ kV + filter, e.g., bones in diagnostics, rocks in materials science, etc.) can be used.

In the CT technique, the so-called CT number is used (Hounsfield unit, HU), which indicates the absorption compared to water: $\text{HU} = 1000 \times (\mu\text{-}\mu_{\text{water}}) / (\mu_{\text{water}} - \mu_{\text{air}})$. The CT number provides a clear way of identification of CT scans in addition to in-

dicating the differences for materials with different absorption values. One of the most important requirements for using CT is the ability to measure the absorption of the radiation. This process requires using high-quality detectors.

Various imaging errors may occur during working with CT, caused by several so-called “artifacts”. One of these is beam hardening. Another one can be the appearance of ring artifacts, because of errors of the detector. Several methods and software packages are available to correct such artifacts (Boas & Fleischmann, 2012).

CT examinations generally result in a 2-dimensional image, a “slice” in greyscale. Each pixel in this image contains an HU value, which supplies information on average density and composition of the material in the volume behind the pixel. These 2D slices can be used for 3D reconstructions (Herman, 2009).

2.2. Sample preparation, analysis and visualisation

One of the samples studied here is from the thermal-spring fed Lake Peșea (Lake St Ladislaus) at Băile 1 Mai, north-west Romania, where a geological section of 8.4 m was deepened in 2011 (Sümegei et al., 2012). The other sampling area is the Upper Cretaceous (Santonian) Csehánya Formation at the Iharkút vertebrate locality in the Bakony Mountains, western Hungary (Ósi et al., 2005) (Fig. 1).

Prior to taking measurements, gyrogonites were fixed in 0.2 ml and 1.5 ml PCR tubes, using 20 μl and 100 μl 1% agarose (Strotton et al., 2018). Samples were fixed in a position closest as possible to vertical before scanning; this is important in the subsequent digital sectioning of the slices.

Our samples have been examined with a Bruker Skyscan 2211 Nano-CT cone beam scanner (Szabó et al., 2022) at the Department of Applied and Environmental Chemistry, University of Szeged. Images obtained were reconstructed by using the modified Feldkamp algorithm of the NRecon reconstruction software (Skyscan, Bruker, Belgium). Visualisation and analysis were performed by using the ORS Dragonfly software (Duncan et al., 2022). For leveling, a window with values ranging from 0 to 224.3 and the all-pass constant opacity filtering have been used. When samples are not perpendicular to the main axis of rotation the pitch has to be modified so as to achieve the desired perpendicular view angle in slices. We have also tested how this works with ImageJ. (Schneider et al., 2012). 3D visualisation has been carried out by ImageJ's Volume Viewer



Fig. 1. Location of sampling areas.

plugin using the 'Volume' display mode. Before image processing, micro-CT slice series have been narrowed down to images containing a section of the gyrogonite. These slices were cropped to the maximum extent of the series subject, with suitable border area (such are not mandatory, but highly recommended steps, because they significantly reduce memory usage. It is useful to flip the images before loading them into the CT analysis program to obtain the correct sample orientation.

Histograms of the cropped image stacks have been analysed in order to determine appropriate upper and lower threshold values, which have been used to adjust brightness, increase subject contrast and aid discrimination from background.

Analyses of our gyrogonite samples are presented below.

2.2.1. Sample no. 23/2 from Lake Peřea

The basal part of the gyrogonite analysed was intact, but the apical part was missing and the internal structure was not completely preserved (Fig. 2).

Observed with the naked eye, the gyrogonite has a white colour, while the internal structure is

brown. In general, in fully intact characean remains, gyrogonites are composed of five spiral cells (Haas, 1994). In the present specimen, the spiral cells were only partially preserved. Despite this drawback, these spiral cells are clearly visible and countable in basal view. Their distinctive pattern is also an important feature of descriptions of such remains (Soulié-Märsche & García, 2015).

During examination the following settings have been used on sample no. 23/2: scanner: Bruker Sky-Scan2211, source voltage: 70 kV, source current: 500 μ A, exposure time: 225 ms, image pixel size: 1.50 μ m, micro-focus mode. A total of 1,940 X-ray images have been created by rotating the sample with an angular step of 0.1° for 3.5 h.

2.2.2. Samples nos. 1A9 and 3C7 from the Csehbánya Formation at Iharkút

When examined under a standard binocular, the colour of the gyrogonites is yellowish white; five convex spiral cells can be seen. Although surfaces are eroded, the basal and apical parts remain intact (Fig. 3).

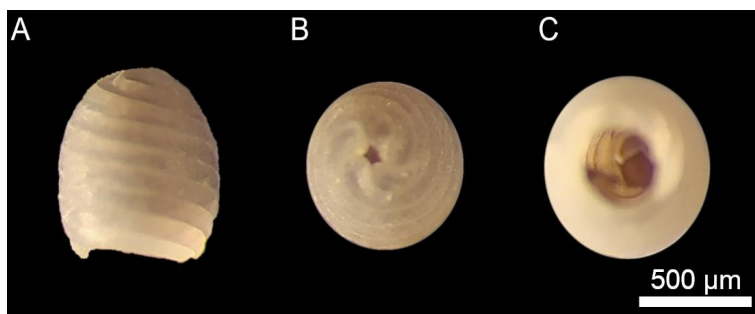


Fig. 2. Sample no. 23/2 in lateral (A), basal (B) and apical (C) view, observed under the microscope.

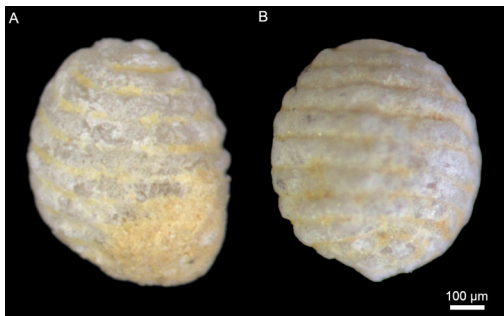


Fig. 3. Samples no. 1A9 (A) and 3C7 (B) in lateral view, observed under the microscope.

With these samples the following settings were used: no. 1A9: Bruker SkyScan2211, source voltage: 70 kV, source current: 700 μ A, exposure time: 600 ms, image pixel size: 0.70 μ m, micro-focus mode. A total of 1,940 X-ray images have been created by rotating the sample with an angular step of 0.1° for 4h 54min. Sample no. 3C7: scanner: Bruker SkyScan2211, source voltage: 60 kV/ 70 kV source current: 476 μ A/ 700 μ A, exposure time: 275 ms/ 400 ms, image pixel size: 1.50 μ m/ 0.70 μ m, micro-focus mode. In total, 1,940 X-ray images have been created by rotating the sample with an angular step of 0.1° for 3 h 40 min and 4 h 50 min.

3. Results and conclusions

In sample no. 23/2 the simple pentagonal basal plate observed under the microscope is also clearly visible in the CT images. Its shape is typical of that of characeans (Soulié-Märsche & García, 2015) (Fig. 4). In contrast to the microscopic images, the basal plate could be studied from several directions on the corresponding 2D slices and 3D models prepared from the CT images (Fig. 5).

It was possible to visualise the specimen in 3D, rotate it, and observe it from different directions. Slicing the 3D model and zooming into various areas has allowed to study tiny structural and ornament patterns inside the specimen as well, in contrast to simple microscopic views where only the superficial morphology can be assessed, at much lower resolutions. It is clearly visible that the outside perimeter of the gyrogonite is composed of higher density material, which may suggest that various mineralogical processes have taken place during its formation.

One main factor in the case of the Iharkút samples is that the inner carbonate material does not show a density that is very different from the exter-

nal part and the beam hardening effect that causes concentric circles to appear (Fig. 6). Thus, it is probably not possible to segment the inner part of the gyrogonite from the external structure, even with SEM. The section clearly shows the spiral creases can be digitised with contour analysis morphology and the shape differences can be analysed

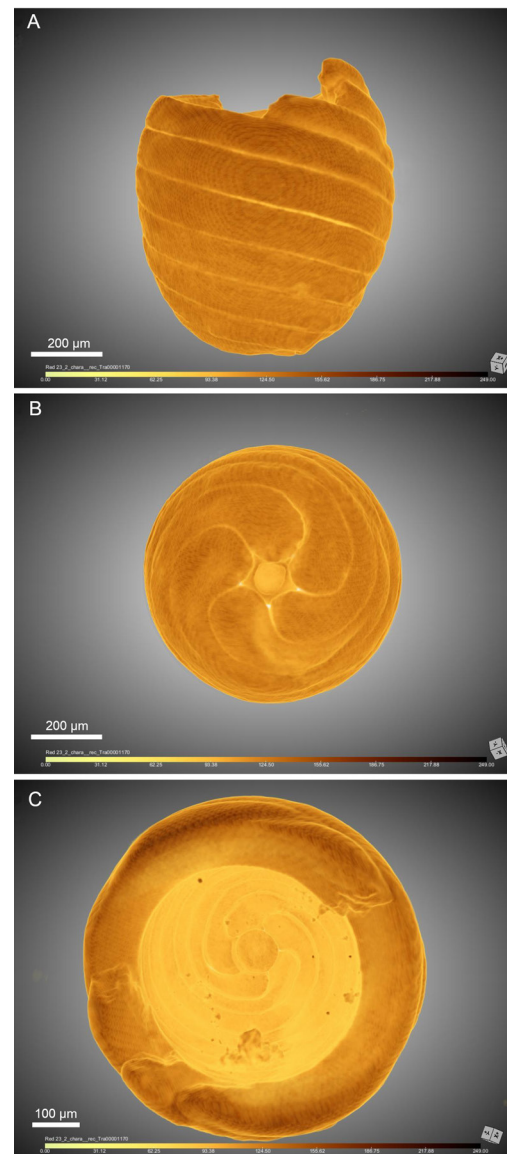


Fig. 4. 3D models of sample no. 23/2 in lateral (A), basal (B) and apical (C) views, prepared from CT images (ORS Dragonfly).

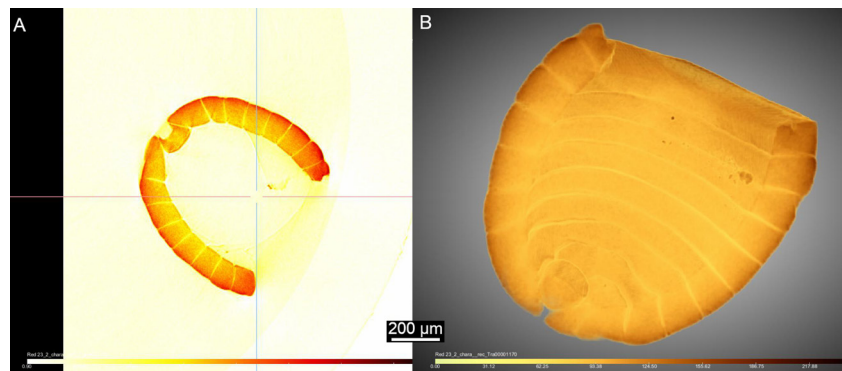


Fig. 5. 2D slice (A) and 3D model (B) of sample no. 23/2 in lateral view (ORS Dragonfly).

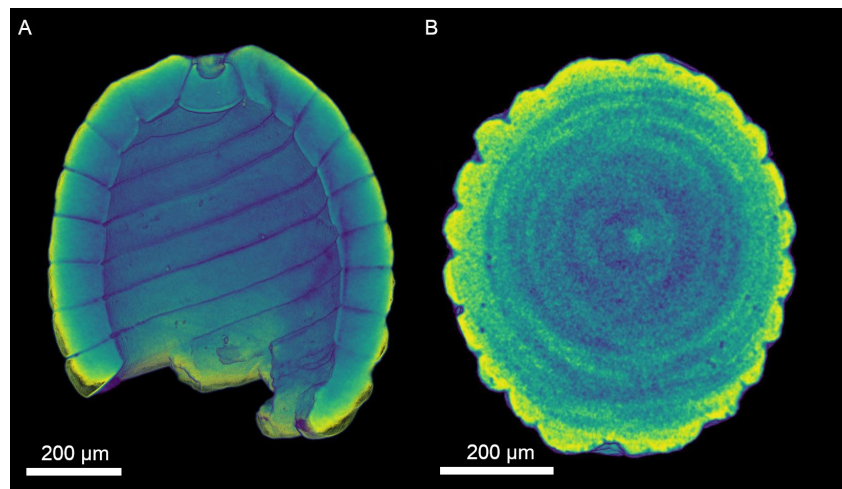


Fig. 6. Difference between lateral sections of samples no. 23/2 (A) and no. 3C7 (B) (3D visualisation by ImageJ).

in more detail than with distance measurements. The analysis can also be used to investigate some of the damage and distortions in the structure of gyrogonites. It is possible to distinguish effectively at which stage of the fossilisation process the dam-

age had occurred (Fig. 7). It is also possible to put in measuring points that are positionally matched and analyse the shape with geometric morphometry. However, measuring points can be also placed not only in 2D but also in 3D on the surface, af-

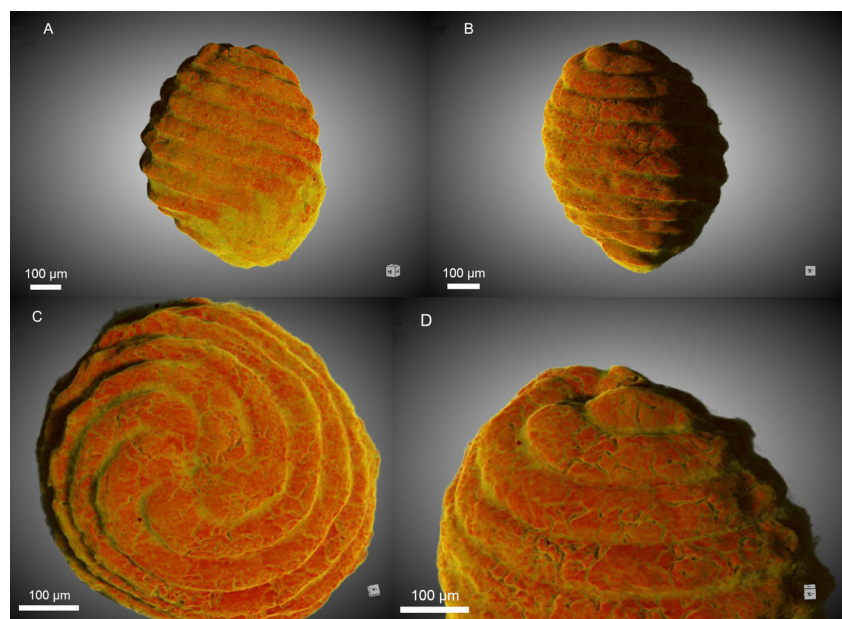


Fig. 7. 3D models of sample no. 1A9 in lateral (A, B) and basal (C, D) views, prepared from CT images (ORS Dragonfly).

ter which 3D geometric morphometry can be done (Fig. 8).

As we have mentioned above, samples were fixed in 0.2 ml and 1.5 ml PCR tubes. The 1.5 ml PCR tubes have been chosen because they were considered more manageable due to their larger volume. However, measurements have shown that the geometry of the sample holder limits the resolution achieved (through the sample-detector distance), so it is advisable to capture the sample in as small a space as possible.

Based on our results so far, micro-CT-based analysis has many advantages and disadvantages. The advantage is that it is non-destructive, which is definitely important for holotypes. One disadvan-

tage is that it is time consuming (preparation and measurements, due to small size, take 5–6 hours). In addition, more than 2,000 slices for high resolution are needed; this yields a huge file size which requires sufficient hardware (large memory and advanced graphics card; at least 6GB memory NVidia GTX or RTX series) and software could be expensive. For this reason, we also recommend to test ImageJ, because it uses less of our hardware and is freely available. The third disadvantage is the price if you need a statistically meaningful number of samples. However, one of the most important advantages of CT images, be they 2D slices or 3D models, is the colour depiction of density differences, which allows the identification of minute differences in the structural composition of certain parts. Density values may also reflect the availability of dissolved chemical components in the water used for the construction of the gyrogonite. Finally, as there is a data set behind the visualised CT images reflecting these compositional (density) differences when more specimens are studied from various habitats and or samples, similarities and differences between them can be assessed via statistical analysis of CT data (cluster analysis, multivariate ordination), thus complementing observations of morphological features. When other geochemical analytical results are also added, these may serve as palaeoecological proxies as well.

Acknowledgements

We wish to thank Emese Bodor (Department of Palaeontology, Institute of Geography and Earth Sciences, ELTE Eötvös Loránd University, Budapest) for the samples from Iharkút. We are grateful to Lívia Vásárhelyi and the Department of Applied and Environmental Chemistry, University of Szeged for the assistance in micro-CT scanning and we would like to thank Ákos Kukovecz for the opportunity. We wish to acknowledge NKFIH Grant 129265 for their support. The manuscript was considerably improved by valuable comments from two anonymous reviewers.

References

- Boas, F. E.; Fleischmann, D., 2012. CT artifacts: causes and reduction techniques. *Imaging in Medicine* 4, 229–240.
- Duncan K.E., Czymmek, K.J., Jiang, N., Thies, A.C. & Topp, C.T., 2022. X-ray microscopy enables multiscale high-resolution 3D imaging of plant cells, tissues, and organs. *Plant Physiology* 188, 831–845.
- Haas, J.N., 1994. First identification key for charophyte oospores from central Europe. *European Journal of Phycology* 29, 227–235.

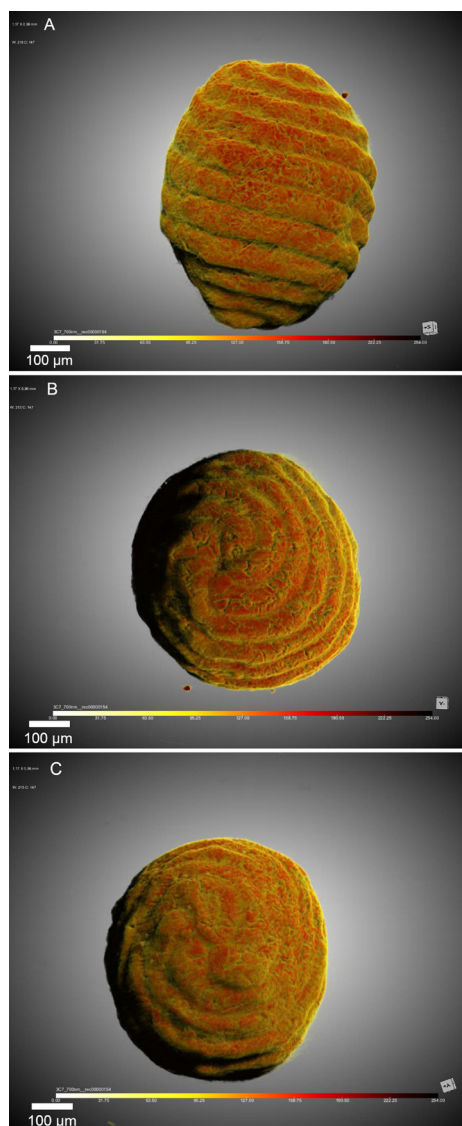


Fig. 8. 3D models of sample no. 3C7 in lateral, basal and apical views, prepared from CT images (ORS Dragonfly).

- Herman, G.T., 2009. *Fundamentals of computerized tomography: Image reconstruction from projection*. 2nd ed., Springer, 300 pp.
- Hounsfield, G.N., 1973. Computerized transverse axial scanning (tomography). 1. Description of system. *British Journal of Radiology* 46, 1016–1022.
- Ósi, A., Weishampel, D.B. & Jianu, C.M., 2005. First evidence of azhdarchid pterosaurs from the Late Cretaceous of Hungary. *Acta Palaeontologica Polonica* 50, 777–787.
- Schneider, C.A., Rasband, W.S. & Eliceiri, K.W., 2012. NIH Image to ImageJ: 25 years of image analysis. *Nature Methods* 9, 671–675.
- Soulié-Märsche, I. & García, A., 2015. Gyrogonites and oospores, complementary viewpoints to improve the study of the charophytes (Charales). *Aquatic Botany* 120, 7–17.
- Strotton, M.C., Bodey, A.J., Wanelik, K., Darrow, M.C., Medina, E., Hobbs, C., Rau, C. & Bradbury, E.J., 2018. Optimising complementary soft tissue synchrotron X-ray microtomography for reversibly-stained central nervous system samples. *Scientific Reports* 8, 12017.
- Sümeği, P., Molnár, D., Sávai, S. & Gulyás, S., 2012. Malacofauna evolution of the Lake Peşea (Püspökfürdő), Oradea region, Romania. *Nymphaea, Folia naturae Bihariae* 39, 5–29.
- Szabó, M., Kundrata, R., Hoffmannova, J., Németh, T., Bodor, E., Szenti, I., Prosvirov, A.S., Kukovecz, Á. & Ósi, A., 2022. The first mainland European Mesozoic click-beetle (Coleoptera: Elateridae) revealed by X-ray micro-computed tomography scanning of an Upper Cretaceous amber from Hungary. *Scientific Reports* 12, 24.
- Tafforeau, P., Boistel, R., Boller, E., Bravin, A., Brunet, M., Chaimanee, Y., Cloetens, P., Feist, M., Horszowska, J., Jaeger, J.-J., Kay, R. F., Lazzari, V., Marivaux, L., Nel, A., Nemoz, C., Thibault, X., Vignaud, P. & Zabler, S., 2006. Applications of X-ray synchrotron microtomography for non-destructive 3D studies of paleontological specimens. *Applied Physics A* 83, 195–202.

Manuscript submitted: 28 April 2022

Revision accepted: 23 May 2023